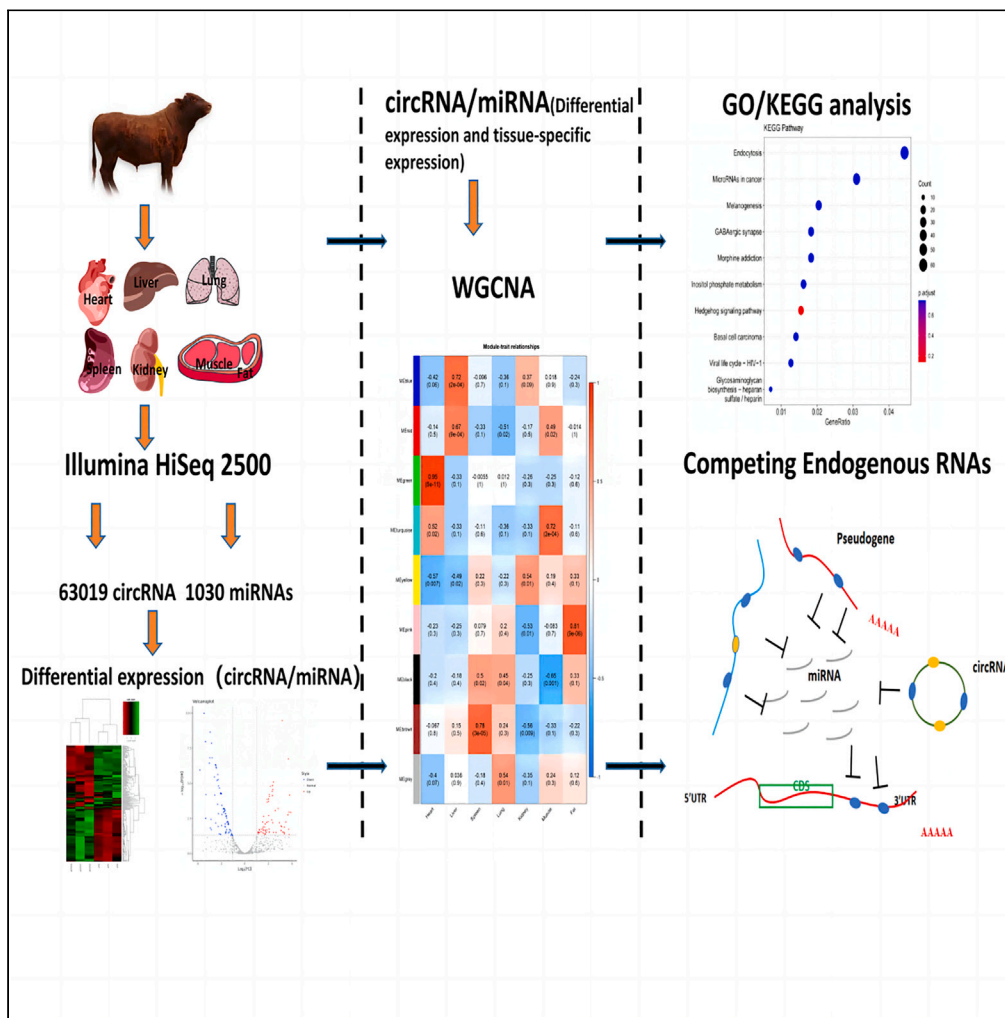# iScience

Article

Construction of a molecular regulatory network related to fat deposition by multi-tissue transcriptome sequencing of Jiaxian red cattle

Shuzhe Wang,
Cuili Pan, Hui
Sheng, ..., Xue
Feng, Chunli Hu,
Yun Ma

mayun_666@126.com

Highlights

Intramuscular fat deposition plays a crucial role in the meat quality of Jiaxian red cattle

RNA-Seq identifies non-coding RNAs in various tissues of Jiaxian red cattle

DE analysis and WGCNA profiling unveil non-coding RNAs relevant to adipose function

Construct a non-coding RNA competitive binding network influencing adipose deposition

iScience

Article

Construction of a molecular regulatory network related to fat deposition by multi-tissue transcriptome sequencing of Jiaxian red cattle

Shuzhe Wang,[1] Cuili Pan,[1] Hui Sheng,[1] Mengli Yang,[1] Chaoyun Yang,[2] Xue Feng,[1] Chunli Hu,[1] and Yun Ma[1,3,*]

SUMMARY

Intramuscular fat (IMF) refers to the fat that accumulates between muscle bundles or within muscle cells, whose content significantly impacts the taste, tenderness, and flavor of meat products, making it a crucial economic characteristic in livestock production. However, the intricate mechanisms governing IMF deposition, involving non-coding RNAs (ncRNAs), genes, and complex regulatory networks, remain largely enigmatic. Identifying adipose tissue-specific genes and ncRNAs is paramount to unravel these molecular mysteries. This study, conducted on Jiaxian red cattle, harnessed whole transcriptome sequencing to unearth the nuances of circRNAs and miRNAs across seven distinct tissues. The interplay of these ncRNAs was assessed through differential expression analysis and network analysis. These findings are not only pivotal in unveiling the intricacies of fat deposition mechanisms but also lay a robust foundation for future research, setting the stage for enhancing IMF content in Jiaxian red cattle breeding.

INTRODUCTION

Non-coding RNAs (ncRNAs) possess a wide range of crucial biological functions, encompassing the regulation of gene expression at multiple levels, including transcription, RNA processing, and translation.[1,2] Recent research has demonstrated that the regulation of fat deposition involves a diverse array of ncRNAs and transcription factors.[3] For example, *circFUT10* has emerged as a fascinating case, as it not only enhances adipocyte proliferation but also inhibits differentiation by acting as a sponge for *let-7*.[4] In a different context, exosomal *circ133* has been found to drive the browning of white fat by directly influencing the *miR-133*/PRDM16 pathway.[5] Furthermore, *circ09863* regulated unsaturated fatty acid metabolism in bovine mammary epithelial cells by competitively binding to *miR-27a-3p*.[6] The interaction of ncRNAs is one of the key steps in the control of gene expression, determining the final protein output in a hierarchical (circRNA-miRNA-mRNA-protein) system.

The versatility of ncRNAs confers multiple roles on the RNA complex, ranging from controlling RNA transcription to competing for binding with target sequences.[7,8] Most circRNAs contain multiple binding sites and can thus target multiple miRNAs, while a single miRNA can also interact with multiple circRNAs to form a complex competing endogenous RNA (ceRNA) network in addition to targeting the 3′UTR of multiple mRNAs.[9] Previous studies mainly identified ncRNAs based on different conditions in single tissue, such as cancer production,[10] breast lesions,[11] adipose differentiation,[12] and alcoholic fatty liver.[13] In addition, ncRNAs could be identified from different varieties (e.g., human with bovine)[14] or from multiorganization (e.g., muscle and fat).[15] Nevertheless, the transcriptome of different tissues varied under different physiological and pathological conditions. Studying just one tissue limits our understanding of diverse biological processes, and focusing on single-tissue sequencing overlooks complex tissue interactions. Conducting RNA sequencing across multiple tissues offers a holistic view, revealing tissue-specific genes and regulatory mechanisms.

Accurately identifying of ncRNAs and their regulatory networks required a comprehensive study of different tissues. Various tissues usually communicate with each other to coordinate the regulation of growth, development and metabolism. Therefore, it is crucial to gain a deeper understanding of the regulatory relationships between adipose and other tissues. In this study, adipose tissue and six tissues (heart, liver, spleen, lung, kidney, and muscle) closely related to it were selected for sequencing. The liver and fat exhibit a tightly regulated relationship, forming a liver-fat regulatory axis. Glucocerebrosidase enzymes in the liver govern glucose synthesis and release, while lipocalin in adipose tissue modulates insulin sensitivity and energy metabolism.[16] Intramuscular fat (IMF) can alter the tenderness and flavor of beef, and the process of IMF production is an important direction in the study of the relationship between muscle and fat.[17] Excessive lipid synthesis leads to the accumulation of cholesterol in the arteries and the formation of cardiac fat around the heart.[18] Excess fat also reduces the compliance of
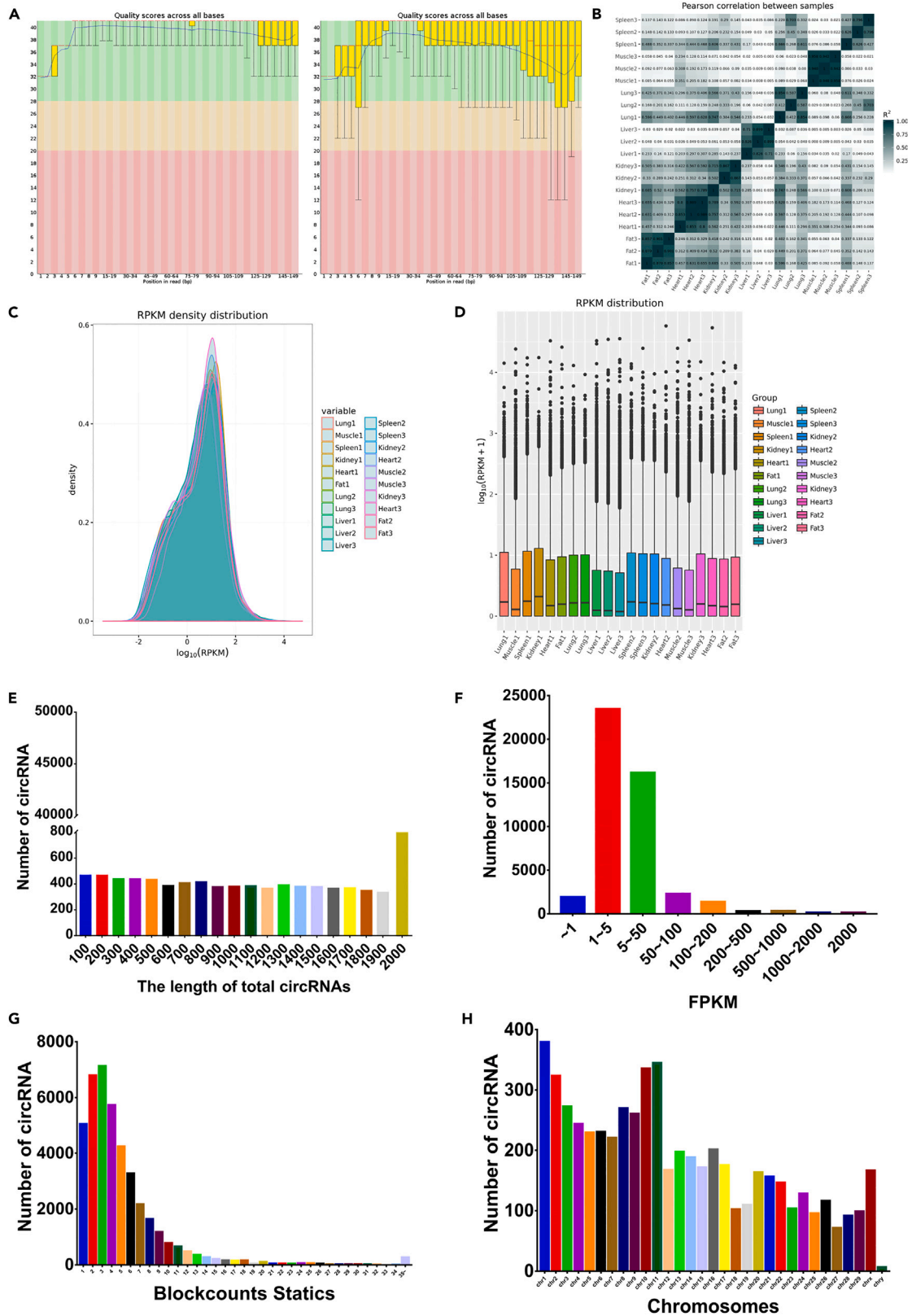
Figure 1. Identification and characteristic analysis of circRNA in heart, liver, spleen, lung, kidney, muscle, and fat of Jiaxian Red Cattle

(A) Original read quality control.

(B) Pearson correlation coefficient analysis between different organizations.

(C) RPKM density distribution.

(D) RPKM expression pattern.

(E) CircRNAs length distribution.

(F) Statistics on the number of circRNAs identified in bovine skeletal muscle with tail shear reads.

(G) CircRNA contains Exon number statistics.

(H) The distribution of circRNAs in different chromosomes of cattle.

the entire respiratory system, and increased lung resistance, resulting in an increased risk of disease.[19] In addition, it can also be deposited around the spleen and kidney, leading to organ damage and metabolic diseases.[20] Clarifying the regulatory relationships between the heart, liver, spleen, lung, kidney, muscle, and fat tissues is essential to understanding the mechanisms of adipose tissue metabolism. Therefore, we conducted a comprehensive analysis of ncRNA in these seven different tissues (heart, liver, spleen, lung, kidney, muscle, and adipose) to provide insight into the molecular mechanisms associated with fat deposition.

The Jiaxian red cattle is an excellent local yellow cattle breed in China, whose meat is tender and marbling is obvious. Improving meat quality in this breed is of utmost importance. This study employed tissue-specific differential expression analysis, gene co-expression network analysis (WGCNA), and comprehensive screening to identify key circRNAs and miRNAs involved in fat development in Jiaxian red cattle. Consequently, a molecular regulatory network was constructed, contributing to a deeper understanding of fat deposition and carrying significant implications for the breeding and enhancement of meat quality in Jiaxian red cattle.

RESULTS

Multi-tissue circRNA identification of Jiaxian red cattle

21 samples were collected from seven different tissues of three cattle to construct ribosome-depleted RNA libraries, enabling the identification of circRNA expression data. Polished version: The RNA libraries yielded a total of 1,848,999,744 reads, which underwent quality control and filtering to remove low-quality reads (Figure 1A), the remaining reads were then aligned to the genome (Table S1). Through comprehensive analysis, a total of 63,019 circRNAs were identified, with 18,321 circRNAs originating from a single back-spliced read. Intriguingly, the remaining circRNAs either showed partial distribution across 2–5 tissues or were exclusive to a single tissue, with only 7,980 circRNAs exhibiting presence across all seven tissues. The Pearson coefficients of expression levels between tissues converged to 1, indicating normal gene expression patterns in the tissues (Figures 1B–1D). The large sample size resulted in a substantial number of long circRNAs (>1000 bp) (Figure 1E). However, most circRNAs exhibited low expression levels, with less than five supporting back-spliced reads (Figure 1F). The analysis of circRNA sequence structures showed that highly expressed circRNAs had a consistent number of exons across diverse tissues, usually ranging from 2 to 10 exons. However, it is worth noting that only a minority (5%) of circRNAs comprised a single exon (Figure 1G). The majority of circRNAs are derived from reverse splicing of one or multiple exons within a gene. Chromosomal distribution analysis revealed a widespread and relatively uniform distribution of circRNAs across all chromosomes. Longer chromosomes have a higher potential for generating reverse splicing sites, leading to the production of more circRNAs (Figure 1H). Additionally, the analysis results suggested that a single parental gene could generate multiple circRNA isoforms, such as 1–5 circRNAs (Figure S1A). Notably, only 1–2 circRNAs typically exhibit the higher expression levels (Figures S1B–S1D).

Multi-tissue miRNA identification of Jiaxian red cattle

A dedicated small RNA library was created, resulting in a total of 467,209,612 reads from all tissue samples. Quality filtering was applied to remove low-quality reads (Figure 2A), and the resulting clean reads were aligned against the miRbase database (Table S2). Unmapped reads that did not match the miRbase database were then aligned to the cattle genome to identify potential novel miRNAs (Table S3). A total of 1,030 candidate miRNAs were identified, but unfortunately, no new miRNAs were discovered. Analysis revealed high Pearson correlation coefficients indicating similar expression levels among tissues, and the gene expression patterns within tissues were normal (Figures 1B–1D). Further analysis of miRNA sequence characteristics showed a preference for U as the first base of mature miRNAs (Figure 2E), and the lengths of miRNAs ranged from 16 to 24 bp, consistent with typical miRNA features (Figure 2F).

Differential expression analysis of circRNAs and miRNAs in Jiaxian red cattle

Differential expression analysis of circRNAs and miRNAs was performed in six different tissues compared to adipose tissue. Significant expression patterns were observed in each tissue: the heart had 392 upregulated and 277 downregulated circRNAs, along with 91 upregulated and 80 downregulated miRNAs; the liver showed 346 upregulated and 487 downregulated circRNAs, with 132 upregulated and 82 downregulated miRNAs. In the spleen, there were 427 upregulated and 155 downregulated circRNAs, along with 58 upregulated and 75 downregulated miRNAs. The lungs exhibited 451 upregulated and 182 downregulated circRNAs, with 63 upregulated and 72 downregulated miRNAs. Kidneys had 373 upregulated and 283 downregulated circRNAs, along with 120 upregulated and 43 downregulated miRNAs. Finally, muscles showed
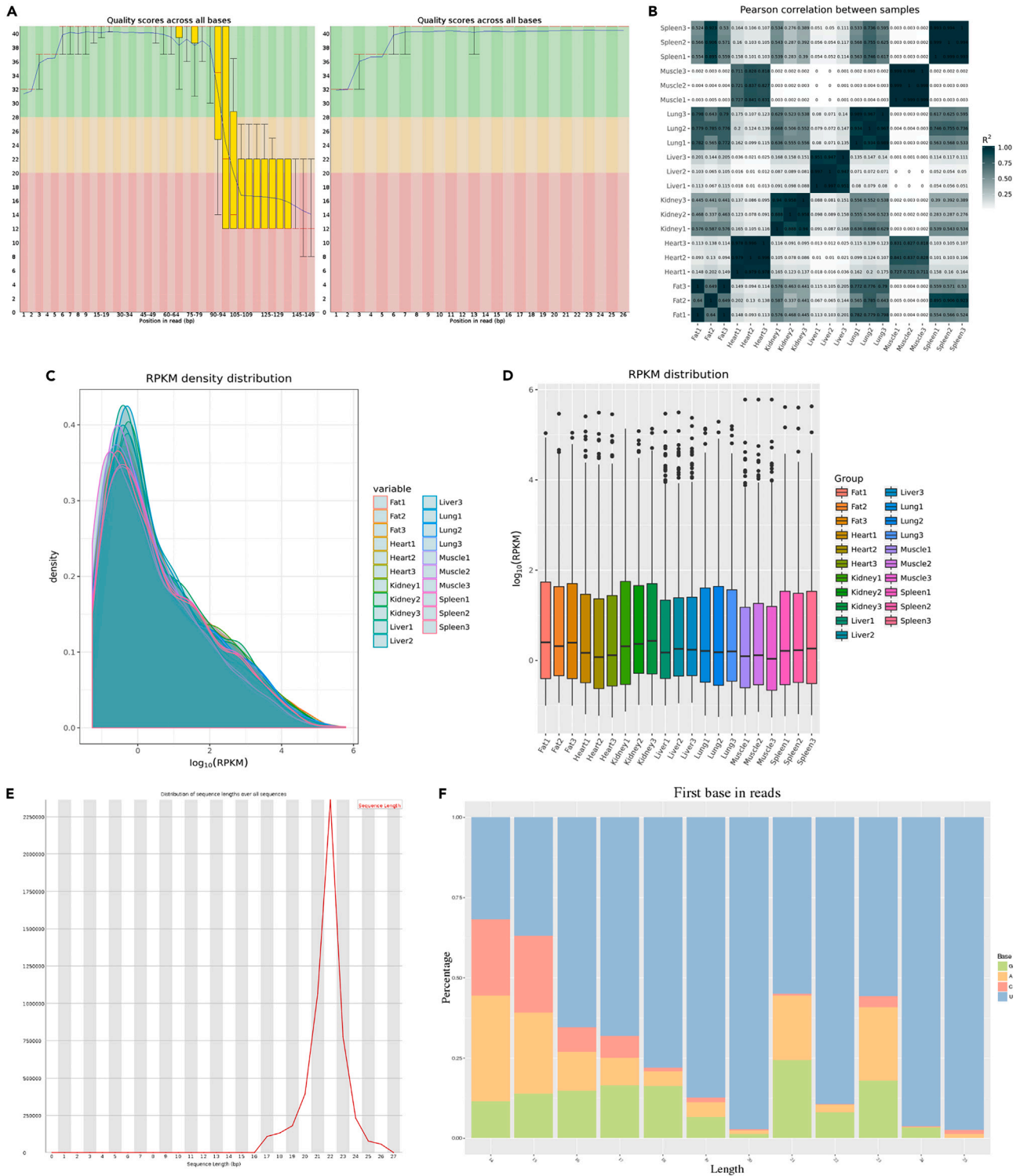
Figure 2. Identification and characteristic analysis of miRNAs in bovine heart, liver, spleen, lung, kidney, muscle, and fat

(A) Original read quality control.

(B) Pearson correlation coefficient analysis between different organizations.

(C) RPKM density distribution.

(D) RPKM expression pattern.

(E) miRNAs length distribution.
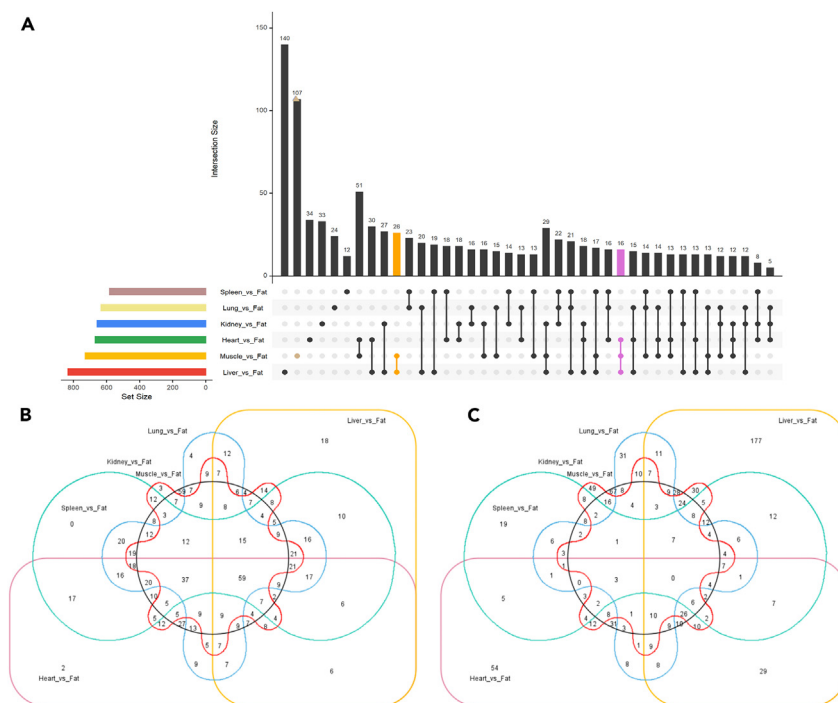
(F) miRNA first base preference.

Figure 3. Differential expression analysis of circRNAs

(A) Upset analysis of differentially expressed circRNAs.

(B) Upregulation of differentially expressed circRNAs by venn analysis.

(C) Downregulation of circRNAs venn analysis.

407 upregulated and 321 downregulated circRNAs, along with 87 upregulated and 64 downregulated miRNAs. (Figures 3 and 4A, and Table S4).

Comparative venn analysis, using adipose tissue as a control, revealed upregulated circRNAs in various tissues. Notable circRNAs, including *circKCNN2*, *circCANX*, *circFAM129B*, *circARHGAP29*, *circSERINC2*, and *circHHAT*, were significantly elevated in adipose tissue. Some circRNAs in the lungs and muscles also showed differential expression but not significantly higher than other tissues (Figures 3B and 3C). Additionally, the analysis of differentially expressed miRNAs identified various miRNAs with upregulation in specific tissues, such as *miR-30a-5p* in the heart, liver, and kidneys, and *miR-29d-3p* in multiple tissues. Conversely, some miRNAs, like *miR-30c*, *miR-30d*, *miR-9-3p*, *let-7f*, *miR-214*, and *miR-129*, were downregulated in multiple tissues. Although these miRNAs exhibit tissue-specific expression, their significantly higher levels in adipose tissue suggest their involvement in adipose tissue growth and development. (Figures 4B and 4C).

WGCNA analysis of circRNA and miRNA in Jiaxian red cattle

This study performed WGCNA on 14,639 circRNAs with high relative expression, differential expression, and tissue-specific expression. Clustering analysis of the samples indicated distinct tissue-based distinctions, the circRNA screening employed a soft threshold of 8, resulting in the division of the ncRNA into seven co-expression modules through dynamic cutting and tissue module merging (Figures 5A–5C). The red module, highly associated with muscle tissue, and the blue module, highly associated with adipose tissue, were selected for further analysis based on correlation coefficient magnitude and significance (Figure 5D). Analysis revealed that the tissue-specific circRNAs within the modules were mostly independent, with only a few circRNAs intersecting with differentially expressed genes. The majority of strongly associated circRNAs were tissue-specific. By comparing the WGCNA results with differential expression results using venn analysis, a total of 33 circRNAs potentially involved in adipose-related functions were identified. Notably, circRNAs such as *circANKEF1*, *circADAMTS16*, *circCAP2*, *circZNF292*, *circATP6AP2*, *circDDHD1*, and *circHHATL* exhibited significantly higher expression in adipose tissue.

The study also performed a miRNA gene co-expression network analysis (WGCNA). Clustering analysis of the samples identified seven distinct clusters, each corresponding to a specific tissue type, highlighting tissue type as the primary source of sample functional changes (Figures 6A and 6B). Subsequently, miRNAs within the pink module, strongly linked to adipose tissue, and the turquoise module, closely associated with muscle tissue, were chosen for further investigation (Figures 6C and 6D).
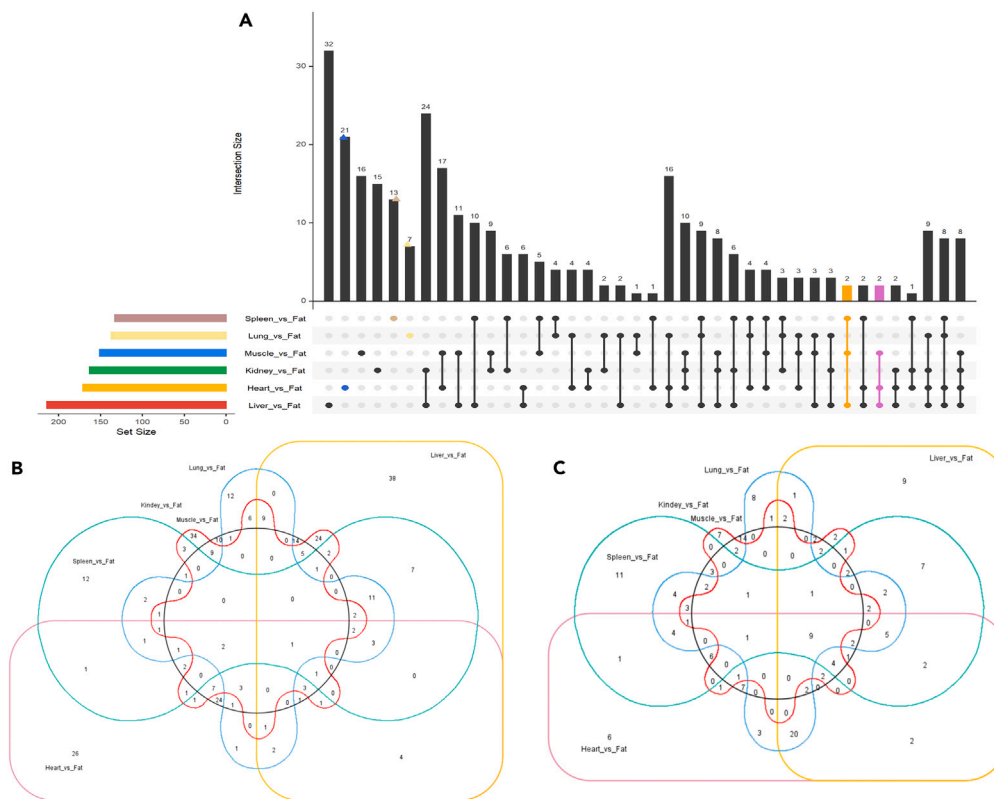
Figure 4. Differential expression analysis of miRNAs

(A) Upset analysis of differentially expressed miRNAs.

(B) Upregulation of differentially expressed miRNAs by venn analysis.

(C) Downregulation of miRNAs venn analysis.

Functional enrichment analysis of target genes and key gene screening

After conducting venn analysis, a total of 74 upregulated miRNAs and 72 downregulated miRNAs were identified by comparing the results of Weighted Gene Co-expression Network Analysis (WGCNA) and differential expression analysis, which included 168 miRNAs. Furthermore, 48 miRNAs were found to be commonly present in both the upregulated and downregulated miRNA sets (Figure 7A).

The target genes of these miRNAs were predicted using TargetScan7.2, RNAhybrid, and miRanda, and venn analysis was performed on the results from these tools. A total of 2,841 target genes and 7,231 miRNA-target gene pairs were identified. Functional enrichment analysis revealed various molecular functions, including catalytic activity, ATP binding, and phosphotransferase activity, among others. Notably, the catalytic activity pathway was enriched with 109 genes, including *CDK5*, *CDK6*, and *CDK12*, which are important transcription factors involved in adipocyte proliferation and apoptosis. Cellular component analysis showed the involvement of 132 genes in different cellular structures such as early endosome membrane, cell surface, and cytoplasmic vesicles. Cytoplasmic vesicles exhibited the highest enrichment, and as adipose-derived extracellular vesicles play a significant role in intercellular communication, the identified target genes are likely to be downstream candidates of miRNAs. Biological process analysis highlighted pathways such as protein-DNA complex assembly, DNA conformation change, and skeletal muscle cell differentiation. The pathway with the highest enrichment was the regulation of body fluid levels, while protein-DNA complex assembly showed the highest confidence level (Figures 7B–7D). The analysis of target genes revealed their enrichment in various disease- and cancer-related signaling pathways, such as endocytosis, microRNAs in cancer, melanogenesis, and morphine addiction. In addition, a few genes were found to be enriched in fat-related signaling pathways like the insulin signaling pathway and AMPK signaling pathway. These findings highlight the importance of exploring miRNAs associated with fat-related signaling pathways as potential candidate ncRNAs (Figure 7E).

The expression of circRNAs was found to be positively correlated with their host genes. Functional annotation and pathway analysis were performed on differentially expressed circRNAs and key circRNAs identified through WGCNA (Figure S3). It was discovered that the gene functions and signaling pathways associated with circRNA host genes differed significantly from those involved in miRNA target gene signaling pathways. Furthermore, RNAhybrid and miRanda were used to predict the interactions between circRNAs and miRNAs. Functional annotation analysis was conducted on tissue-specific circRNAs and their associated miRNAs and mRNAs. The results of target gene prediction for circRNAs were consistent with the analysis of miRNA target genes alone (Figure S4). Many genes related to adipogenesis and
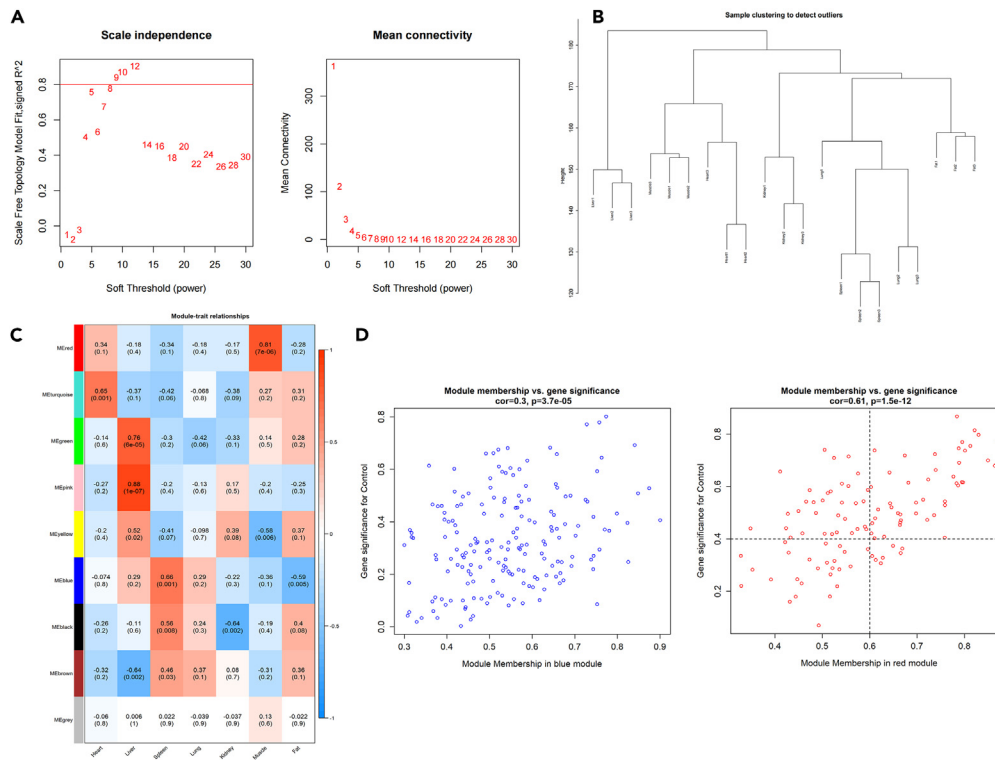
Figure 5. CircRNA WGCNA analysis

(A) To obtain better topological relationships, perform soft thresholding β calculation, in this study β = At this point, R2 is 0.8, and the average connectivity area is constant.

(B) Sample clustering using gene sets for constructing co expression networks.

(C) Analyze the correlation between genes and traits.

(D) The correlation between gene GS and MM values in modules blue and pink indicates a significant correlation between GS and MM.

metabolism pathways were repeatedly identified, facilitating the identification of core ncRNAs related to adipose function and the construction of a circRNA-miRNA-mRNA interaction network.

Predictive analysis of core non-coding RNA and ceRNA network for fat function in Jiaxian red cattle

MiRNAs targeting adipose-related genes were selected, and circRNAs interacting with these miRNAs were identified. Unstable expression and artifact-prone circRNAs were excluded. Separate ceRNA networks related to adipose function were constructed using *circANKEF1*, *circCAP2*, *circKCNN2*, and *circADAMTS16* as cores. *circADAMTS16* interacted with *miR-504*, *miR-329a*, and *miR-493*, which targeted genes involved in insulin metabolism, glycerol synthesis, and other adipose-related functions (Figure 8A). The ceRNA network centered around *circANKEF1* was enriched with functional genes in the MAPK signaling pathway, Apelin signaling pathway, and transforming growth factor β signaling pathway, including *PLIN1* and *MAPK4* (Figure 8B). The miRNAs interacting with *circKCNN2* were primarily associated with the p53 signaling pathway, MAPK pathway, and insulin-related signaling pathways (Figure 8C). The miRNAs targeting *circCAP2* showed strong associations with their target genes, particularly those involved in insulin production and adipocyte cytokine signaling pathways (Figure 8D).

Identification and epigenetic characterization of non-coding RNA

To validate the accuracy of the analysis results, this study randomly selected four differentially expressed circRNAs. Specific primers were designed at the junction sites of circRNAs (Figure S5), and qRT-PCR was performed to measure their expression levels in cattle tissue samples. The quantitative measurements were consistent with the sequencing results (Figures 9A and 9B). Additionally, to determine the expression abundance of miRNAs in different tissues, four differentially expressed miRNAs were randomly selected. Total RNA containing miRNAs was reverse transcribed using loop primers, followed by quantitative PCR using corresponding primers. Comparison of the relative expression levels obtained from miRNA sequencing and qRT-PCR showed a good agreement between the sequencing and quantitative results (Figures 9C and 9D), confirming the accuracy of the sequencing results.

Subsequently, an association analysis was performed between the key ncRNAs selected and the laboratory-generated phenotypic data related to adipose tissue amino acids (Table S5). The results showed significant correlations between *circANKEF1* and Glu and Lys
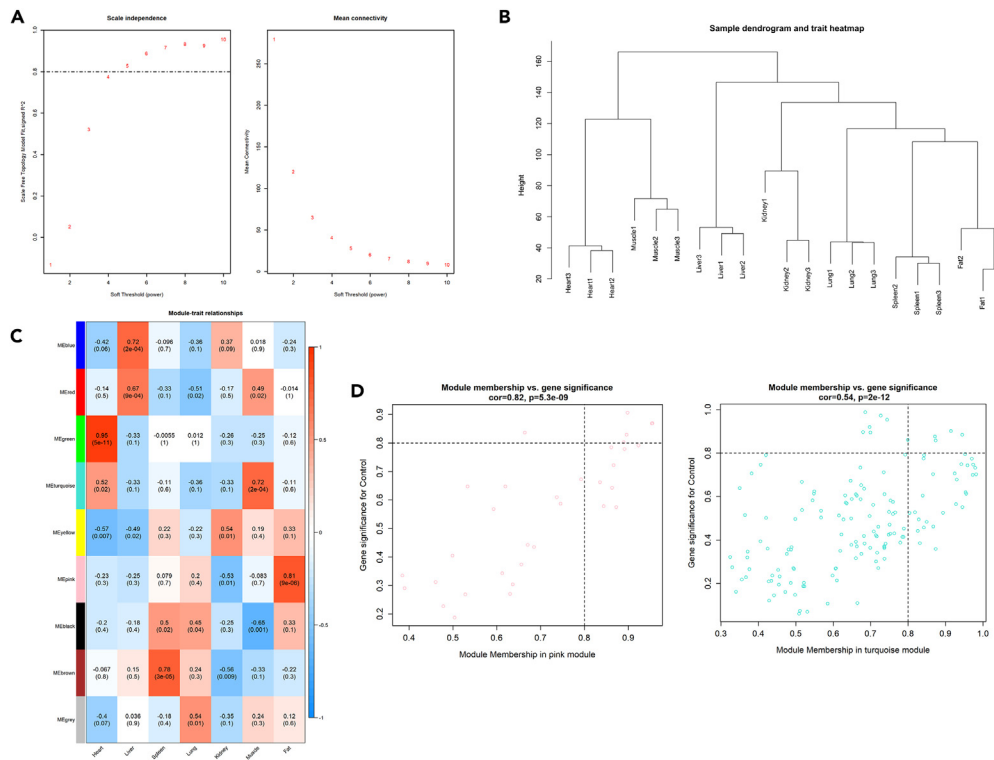
Figure 6. miRNA WGCNA analysis

(A) To obtain better topological relationships, perform soft thresholding β calculation, in this study β = At this point, R2 is 0.8, and the average connectivity area is constant.

(B) Sample clustering using gene sets for constructing co expression networks.

(C) Analyze the correlation between genes and traits.

(D) The correlation between gene GS and MM values in modules blue and pink indicates a significant correlation between GS and MM.

($p < 0.05$), as well as significant correlations between *circKCNN2*, *circCAP2*, and Val, Ile ($p < 0.05$) (Figure 10A). Among the miRNAs, *miR-129* and *miR-127* exhibited significant correlations with Val, Lys, Met, Leu, Pro ($p < 0.05$), while *let-7f* and *miR-29d-3p* showed significant correlations with Gly, Ser, Ala, and other amino acids ($p < 0.05$). The results of the association analysis suggest that these ncRNAs may serve as key candidate genes involved in organismal growth, development, and fat deposition (Figure 10B).

DISCUSSION

MicroRNAs, along with other ncRNAs such as lncRNAs, pseudogenes, and circRNAs, and ceRNAs, play crucial roles in cell-fate determination.[21] Protein-coding messenger RNAs, ncRNAs (such as long ncRNAs, pseudogenes, and circular RNAs), and microRNAs can interact to form complex regulatory networks.[22] Therefore, studies targeting the functional prediction have adopted this idea by first screening for potential miRNAs that interact with circRNAs and then predicting the acting mRNAs of miRNAs. This approach allows for the initial functional analysis of circRNAs and serves as the foundation for constructing circRNA-miRNA-mRNA interaction networks.

Most of the current studies on circRNAs are on shorter circRNAs (<500 bp).[23,24] In this study, we identified long-stranded circRNAs (>800 bp), which have the potential to enrich subsequent functional verification processes. These long-stranded circRNAs exhibit lower protein-coding capacity and form a closed-loop structure, distinguishing them from lncRNAs (long-stranded ncRNAs).[25] Their importance lies in their potential functions within the nucleus, particularly in their role in host gene transcription protection.[26] In addition, the coding function of ncRNAs is also a hot topic of recent research, where circRNAs are able to encode some small peptides.[27] It was speculated that this may be due to the interaction between circRNAs and miRNAs, leading the truncated circRNAs by miRNAs to encode in the cytoplasm.

As is known that circRNAs are generated through reverse splicing, and a single gene can produce 2–8 circRNAs.[28] However, only 1–2 circRNAs among them tend to be highly expressed, while the rest exhibit extremely low or no expression. These low-expressed circRNAs are often ignored in temporal sequencing analyses. However, circRNAs with high expression in a certain tissue might exhibit low or even no expression in another, indicating tissue-specific differential expression.[23] These tissue-specific and differentially expressed circRNAs hold significant value for functional investigations for specific tissue.

miRNA and their regulatory functions have been extensively studied. They showed conservatism between species and tissues.[29] Thus the miRNAs identified are present in one species were generally present in other species. In the study of functional miRNAs of adipose, it was
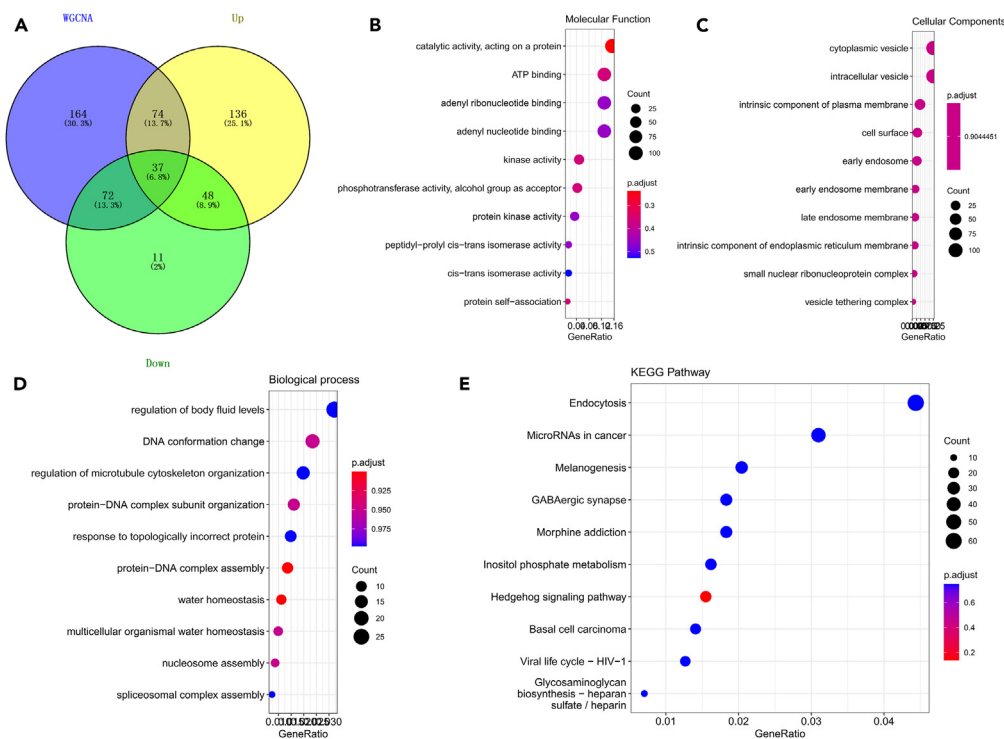
Figure 7. Gene Function Annotation and Signal Pathway Analysis
(A) Wayne analysis of upregulated and WGCNA gene sets, downregulated and WGCNA gene sets, and three gene sets.
(B) GO functional annotation - molecular functional analysis.
(C) GO functional annotation - cell functional analysis.
(D) GO functional annotation - biological functional analysis.
(E) KEGG signaling pathway analysis. (Bubble size represents the number of enriched genes, color represents the confidence level of enriched genes, and the darker the color, the higher the confidence level).

focused on miRNAs with differential expression, especially that are upregulated in in adipose compared to other tissues. miRNAs with high abundance and differentially upregulated in adipose tissue were inferred to play an important role in adipogenesis, adipocyte proliferation and differentiation.

WGCNA is a systems biology method describing gene association patterns between different samples, which could be used to obtain ncRNAs with strong correlation to the target phenotype.[30] In this study, circRNAs and miRNAs were obtained by RNA sequencing of different tissue types, and WGCNA was applied to screen ncRNAs that regulate adipose tissue. The results of differential analysis were then intersected with those of WGCNA analysis for obtaining ncRNAs with higher confidence. However, circRNAs with higher tissue correlation obtained by WGCNA were rarely found in differentially expressed analysis, which might due to the tissue specificity of circRNAs. Fortunately, miRNAs with higher tissue correlation have some intersection with the results of differential expression analysis. For example miR-27b,[31] miR-34a,[32] miR-30a,[33] miR-29d-3p[34] have been proved to play a vital role during adipogenic differentiation.

The annotation of gene functions helps to understand the function and potential modes of action of ncRNAs.[35] CircRNAs are able to interact with parental gene promoters through sequence complementation, ultimately promoting the transcription of genes and triggering positive feedback loops.[36] In addition, circRNAs are also involved in complex networks, in which they compete binding miRNAs (ceRNA networks) to regulate gene function or even the initiation of gene translation.[37,38] Therefore, three annotation approaches were performed in this study, one for circRNA host genes, the other for miRNA target genes, and the third for genes with circRNA-miRNA-mRNA interactions. The function of circRNA host genes discovered through gene annotation is quite different from the gene function of circRNAs involved in ceRNA networks, because the way circRNAs interact with their host genes is mainly as a protective agent to protect the transcription of host genes.[39] Therefore, the adipose-related signaling pathways PPAR pathway,[40] insulin signaling,[41] AMPK pathway[42] and functional ncRNAs (circRNAs and miRNAs) was identified by target gene prediction of within circRNA-miRNA-mRNA network. Ultimately, ceRNA networks related to the function adipose was constructed.

Two methods were used to identify the accuracy of the obtained ncRNAs in adipose function. The traditional method is fluorescence quantitative identification,[43] with results consistent with those expected. This was followed by association analysis[44,45] using phenotypic data with the ncRNAs obtained by screening (circRNA vs. miRNA) for further validation. The amino acid content in beef affects its flavor
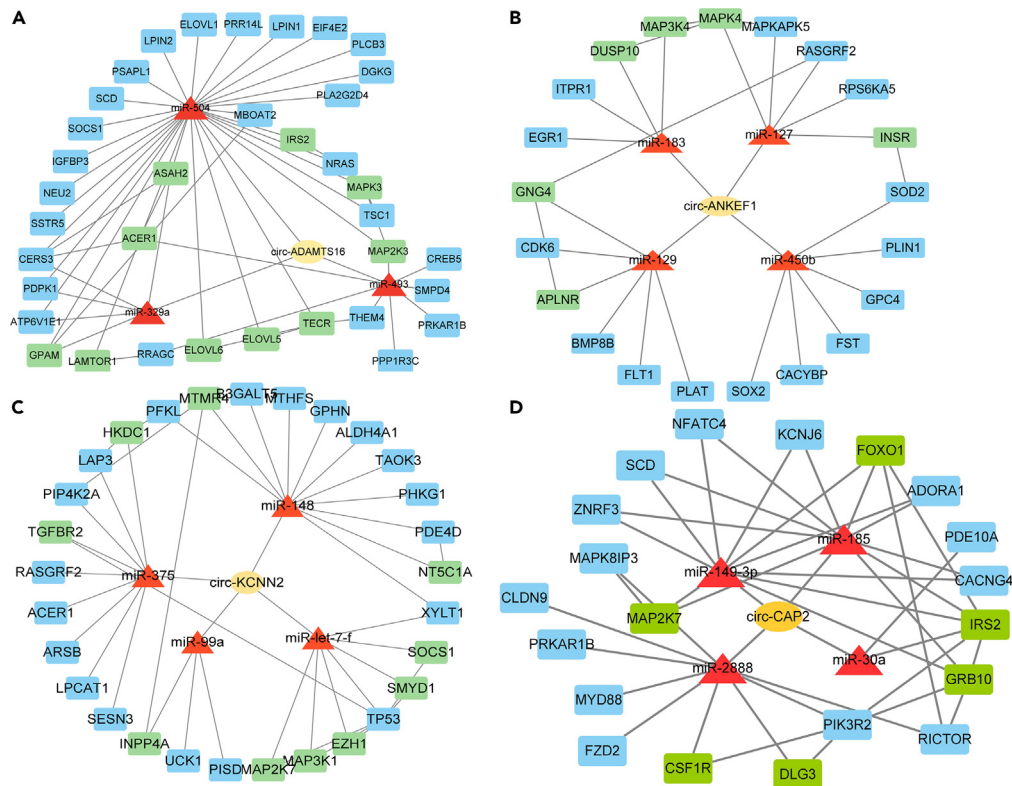
Figure 8. Fat deposition ncRNA competitive binding network
(A) CircADAMTS16 competitive binding network.
(B) CircANKEF1 competitive binding network.
(C) CircKCNN2 competitive binding network.
(D) CircCAP2 competitive binding network. (The yellow circle represents circRNAs, the red triangle represents interacting miRNAs, the rectangle represents mRNA, and the green rectangle represents String displaying interacting mRNA).

and meat quality.[46,47] Correlation analysis was conducted between the amino acid content in beef and the ncRNA obtained through screening, and it was determined that *circANKEF1*, *circCAP2*, *circKCNN2*, *miR129*, *miR127*, *let-7f*, and *miR-29d-3p* can produce key positive and negative regulation in the process of fat generation. And through preliminary laboratory research, it was found that circCAP2 can promote fat generation,[48] *circADAMTS16* can target *miR-10167-3p* to inhibit differentiation of bovine adipocytes but promote proliferation of precursor adipocytes.[49] Other studies have also shown that *miR-129* can inhibit the generation of preadipocytes by targeting *G3BP1*,[50] *let-7f* can participate in WNT signal transduction through multiple pathways,[51] and overexpression of *miR-29d-3p* significantly inhibits genes related to triglyceride synthesis.[34] The aforementioned discussion indicates that the ncRNAs obtained from these analyses are ncRNAs that can play a crucial role in the process of adipogenesis, and multiple ncRNA critical ceRNA networks related to fat function have been identified.

This study aimed to unravel the molecular mechanisms underlying IMF deposition, a crucial factor influencing meat quality, especially in livestock production. Utilizing whole transcriptome sequencing, the research identified a substantial number of circRNAs and miRNAs across various tissues in Jiaxian Red Cattle. Notably, 35 circRNAs exhibited specific expression in adipose tissue. By employing WGCNA, the study pinpointed 32 circRNAs and 46 miRNAs with potential roles in regulating cattle adipocyte proliferation and differentiation. Key players like circCAP2, circANKEF1, let7 families, miR-29-3p, and miR-127 were identified, forming intricate ncRNA competitive endogenous RNA (ceRNA) networks linked to fat regulation. Functional analysis further connected these target genes to vital adipose-related signaling pathways, including PPAR and insulin regulation. These findings provide valuable insights into the development of cattle adipose tissue, offering a foundation for enhancing IMF in Jiaxian Red Cattle breeding programs.

Limitations of the study

The fact that the genomes of cattle are not subdivided among breeds and that the genomes of this species are still being refined has resulted in our inability to efficiently annotate the most comprehensive set of noncoding RNAs. This problem has caused some inconvenience to our research and it is hoped that more researchers will continue to work on refining the bovine genome.
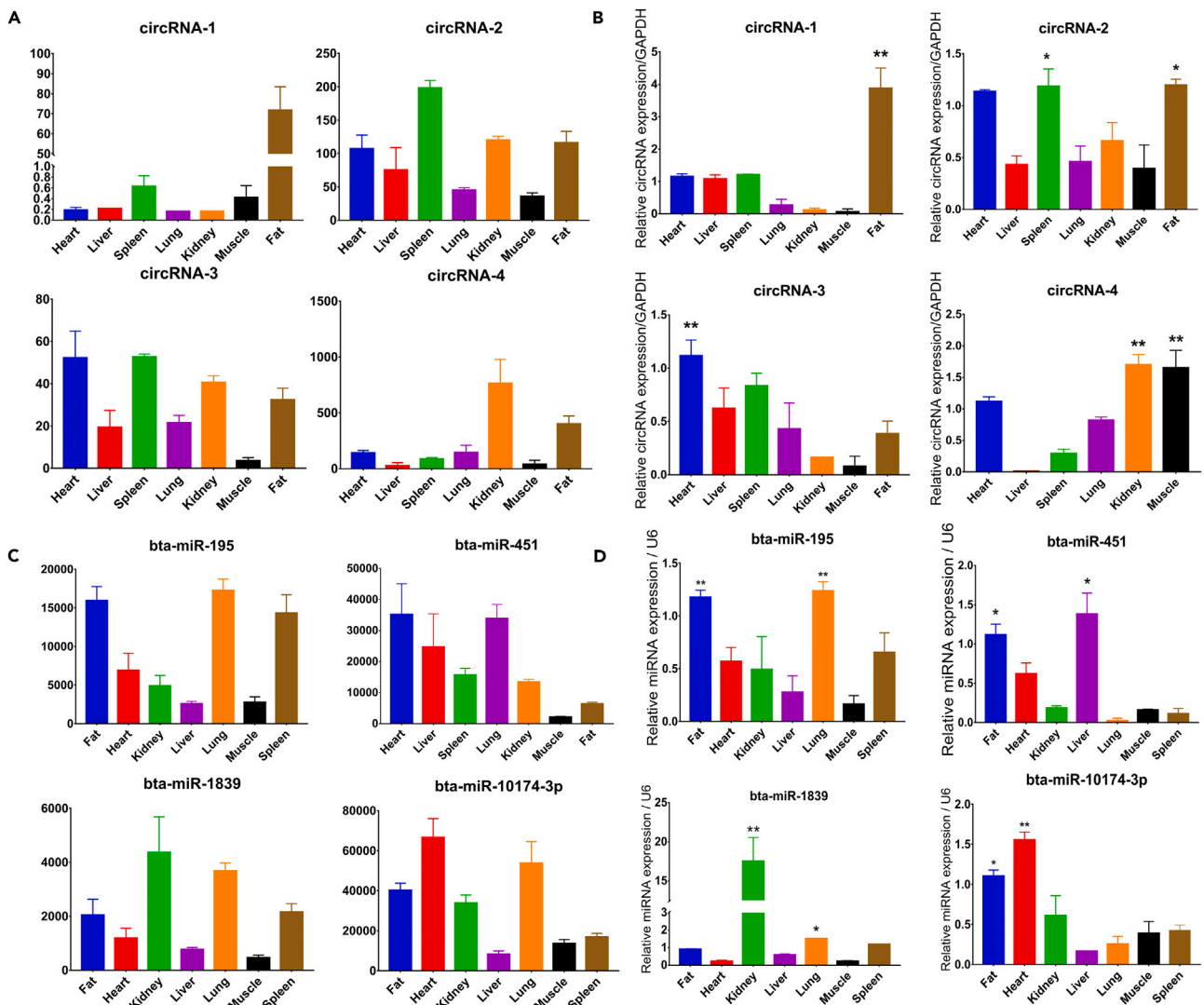
Figure 9. Identification of ncRNA

(A) Analysis of sequencing results of four circRNA expression levels in different tissues.

(B) Real time fluorescence quantitative PCR was used to detect the expression levels of four circRNAs.

(C) Analysis of sequencing results of four miRNA expression levels in different tissues.

(D) Real time fluorescence quantitative PCR was used to detect the expression levels of four miRNAs. (mean $\pm$ SD, n = 3,*p < 0.05. **p < 0.01. ***p < 0.001).

STAR★METHODS

Detailed methods are provided in the online version of this paper and include the following:

- KEY RESOURCES TABLE
- RESOURCE AVAILABILITY
  - Lead contact
  - Materials availability
  - Data and code availability
- EXPERIMENTAL MODEL AND STUDY PARTICIPANT DETAILS
  - Animals
  - Ethics statement
- METHOD DETAILS
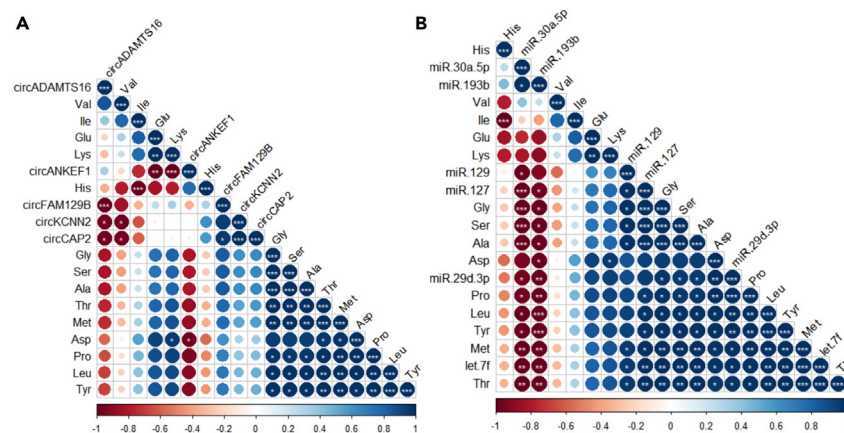 - Sample acquisition and total RNA extraction

Figure 10. Correlation map of ncRNA

(A) Correlation analysis between relative expression levels and amino acids in circRNA fat.

(B) Correlation analysis between relative expression levels and amino acids in miRNA fat. (The darker the legend color, the stronger the correlation, mean ± SD, n = 3, *p < 0.05; **p < 0.01, ***p < 0.001).

- QUANTIFICATION AND STATISTICAL ANALYSIS
  - Identification and differential expression analysis of non-coding RNAs in Jiaxian red cattle
  - Weighted gene co-expression network analysis (WGCNA)
  - Non-coding RNA mechanism prediction and functional enrichment analysis
  - Identification of non-coding RNA by qRT PCR and association analysis with amino acids
  - Statistical tests

SUPPLEMENTAL INFORMATION

Supplemental information can be found online at https://doi.org/10.1016/j.isci.2023.108346.

AUTHOR CONTRIBUTIONS

Y.M., S.W., and C.P. conceived and designed the research. S.W. and C.P. analyzed the data and conducted the experiments. S.W. wrote the manuscript. Y.M., C.H., C.Y., X.F., and H.S. modified the manuscript. All the authors read and approved the final manuscript.

DECLARATION OF INTERESTS

The authors have declared that no conflict of interest exists.

INCLUSION AND DIVERSITY

We support inclusive, diverse, and equitable conduct of research.

REFERENCES

1. Hansen, T.B. (2018). Improved circRNA identification by combining prediction algorithms. Front. Cell Dev. Biol. 6, 20.

2. Diamantopoulos, M.A., Tsiakanikas, P., and Scorilas, A. (2018). Non-coding RNAs: the riddle of the transcriptome and their perspectives in cancer. Ann. Transl. Med. 6, 241.

3. Pirola, C.J., Fernández Gianotti, T., Castaño, G.O., Mallardi, P., San Martino, J., Mora Gonzalez Lopez Ledesma, M., Flichman, D., Mirshahi, F., Sanyal, A.J., and Sookoian, S. (2015). Circulating microRNA signature in non-alcoholic fatty liver disease: from serum non-coding RNAs to liver histology and disease pathogenesis. Gut 64, 800–812.

4. Jiang, R., Li, H., Yang, J., Shen, X., Song, C., Yang, Z., Wang, X., Huang, Y., Lan, X., Lei, C., and Chen, H. (2020). circRNA Profiling Reveals an Abundant circFUT10 that Promotes Adipocyte Proliferation and Inhibits Adipocyte Differentiation via Sponging let-7. Mol. Ther. Nucleic Acids 20, 491–501.

5. Zhang, H., Zhu, L., Bai, M., Liu, Y., Zhan, Y., Deng, T., Yang, H., Sun, W., Wang, X., Zhu, K., et al. (2019). Exosomal circRNA derived from gastric tumor promotes white adipose browning by targeting the miR-133/PRDM16 pathway. Int. J. Cancer 144, 2501–2515.

6. Chen, Z., Zhou, J., Wang, M., Liu, J., Zhang, L., Loor, J.J., Liang, Y., Wu, H., and Yang, Z. (2020). Circ09863 regulates unsaturated fatty acid metabolism by adsorbing miR-27a-3p in bovine mammary epithelial cells. J. Agric. Food Chem. 68, 8589–8601.

7. Guil, S., and Esteller, M. (2015). RNA–RNA interactions in gene regulation: the coding and noncoding players. Trends Biochem. Sci. 40, 248–256.

8. Fabbri, M., Girnita, L., Varani, G., and Calin, G.A. (2019). Decrypting noncoding RNA interactions, structures, and functional networks. Genome Res. 29, 1377–1388.

9. Zhong, Y., Du, Y., Yang, X., Mo, Y., Fan, C., Xiong, F., Ren, D., Ye, X., Li, C., Wang, Y., et al. (2018). Circular RNAs function as ceRNAs to regulate and control human cancer progression. Mol. Cancer 17, 79.

10. Wang, C., Tan, S., Liu, W.-R., Lei, Q., Qiao, W., Wu, Y., Liu, X., Cheng, W., Wei, Y.-Q., Peng, Y., and Li, W. (2019). RNA-Seq profiling of circular RNA in human lung adenocarcinoma and squamous cell carcinoma. Mol. Cancer 18, 134.

11. Wang, X., and Fang, L. (2018). Advances in circular RNAs and their roles in breast Cancer. J. Exp. Clin. Cancer Res. 37, 206.

12. Arcinas, C., Tan, W., Fang, W., Desai, T.P., Teh, D.C.S., Degirmenci, U., Xu, D., Foo, R., and Sun, L. (2019). Adipose circular RNAs exhibit dynamic regulation in obesity and functional role in adipogenesis. Nat. Metab. 1, 688–703.

13. Dou, X., Feng, L., Ying, N., Ding, Q., Song, Q., Jiang, F., Wang, C., and Li, S. (2020). RNA sequencing reveals a comprehensive circular RNA expression profile in a mouse model of alcoholic liver disease. Alcohol Clin. Exp. Res. 44, 415–422.

14. Bush, S.J., Muriuki, C., McCulloch, M.E.B., Farquhar, I.L., Clark, E.L., and Hume, D.A. (2018). Cross-species inference of long non-coding RNAs greatly expands the ruminant transcriptome. Genet. Sel. Evol. 50, 20.

15. Cardoso, T.F., Cánovas, A., Canela-Xandri, O., González-Prendes, R., Amills, M., and Quintanilla, R. (2017). RNA-seq based detection of differentially expressed genes in the skeletal muscle of Duroc pigs with distinct lipid profiles. Sci. Rep. 7, 40005.

16. Luukkonen, P.K., Sädevirta, S., Zhou, Y., Kayser, B., Ali, A., Ahonen, L., Lallukka, S., Pelloux, V., Gaggini, M., Jian, C., et al. (2018). Saturated Fat Is More Metabolically Harmful for the Human Liver Than Unsaturated Fat or Simple Sugars. Diabetes Care 41, 1732–1739.

17. Park, S.J., Beak, S.H., Jung, D.J.S., Kim, S.Y., Jeong, I.H., Piao, M.Y., Kang, H.J., Fassah, D.M., Na, S.W., Yoo, S.P., and Baik, M. (2018). Genetic, management, and nutritional factors affecting intramuscular fat deposition in beef cattle - A review. Asian-Australas. J. Anim. Sci. 31, 1043–1061.

18. Rosenthal, S.B., Bush, K.T., and Nigam, S.K. (2019). A Network of SLC and ABC Transporter and DME Genes Involved in Remote Sensing and Signaling in the Gut-Liver-Kidney Axis. Sci. Rep. 9, 11879.

19. Cornell, K., Alam, M., Lyden, E., Wood, L., LeVan, T.D., Nordgren, T.M., Bailey, K., and Hanson, C. (2019). Saturated Fat Intake Is Associated with Lung Function in Individuals with Airflow Obstruction: Results from NHANES 2007(-)2012. Nutrients 11, 317.

20. Ai, X.M., Ho, L.C., Han, L.L., Lu, J.J., Yue, X., and Yang, N.Y. (2018). The role of splenectomy in lipid metabolism and atherosclerosis (AS). Lipids Health Dis. 17, 186.

21. Li, J.-H., Liu, S., Zhou, H., Qu, L.-H., and Yang, J.-H. (2014). starBase v2. 0: decoding miRNA-ceRNA, miRNA-ncRNA and protein–RNA interaction networks from large-scale CLIP-Seq data. Nucleic Acids Res. 42, D92–D97.

22. Tay, Y., Rinn, J., and Pandolfi, P.P. (2014). The multilayered complexity of ceRNA crosstalk and competition. Nature 505, 344–352.

23. Xia, S., Feng, J., Lei, L., Hu, J., Xia, L., Wang, J., Xiang, Y., Liu, L., Zhong, S., Han, L., and He, C. (2017). Comprehensive characterization of tissue-specific circular RNAs in the human and mouse genomes. Brief. Bioinform. 18, 984–992.

24. Xu, S., Zhou, L., Ponnusamy, M., Zhang, L., Dong, Y., Zhang, Y., Wang, Q., Liu, J., and Wang, K. (2018). A comprehensive review of circRNA: from purification and identification to disease marker potential. PeerJ 6, e5503.

25. Huang, A., Zheng, H., Wu, Z., Chen, M., and Huang, Y. (2020). Circular RNA-protein interactions: functions, mechanisms, and identification. Theranostics 10, 3503–3517.

26. Huang, C., Liang, D., Tatomer, D.C., and Wilusz, J.E. (2018). A length-dependent evolutionarily conserved pathway controls nuclear export of circular RNAs. Genes Dev. 32, 639–644.

27. Wu, P., Mo, Y., Peng, M., Tang, T., Zhong, Y., Deng, X., Xiong, F., Guo, C., Wu, X., Li, Y., et al. (2020). Emerging role of tumor-related functional peptides encoded by lncRNA and circRNA. Mol. Cancer 19, 22.

28. Patop, I.L., Wüst, S., and Kadener, S. (2019). Past, present, and future of circ RNA s. EMBO J. 38, e100836.

29. Lee, C.-T., Risom, T., and Strauss, W.M. (2007). Evolutionary conservation of microRNA regulatory circuits: an examination of microRNA gene complexity and conserved microRNA-target interactions through metazoan phylogeny. DNA Cell Biol. 26, 209–218.

30. Langfelder, P., and Horvath, S. (2008). WGCNA: an R package for weighted correlation network analysis. BMC Bioinf. 9, 559.

31. Karbiener, M., Fischer, C., Nowitsch, S., Opriessnig, P., Papak, C., Ailhaud, G., Dani, C., Amri, E.Z., and Scheideler, M. (2009). microRNA miR-27b impairs human adipocyte differentiation and targets PPARgamma. Biochem. Biophys. Res. Commun. 390, 247–251.

32. Fan, C., Jia, L., Zheng, Y., Jin, C., Liu, Y., Liu, H., and Zhou, Y. (2016). MiR-34a Promotes Osteogenic Differentiation of Human Adipose-Derived Stem Cells via the RBP2/NOTCH1/CYCLIN D1 Coregulatory Network. Stem Cell Rep. 7, 236–248.

33. Guo, Z., Zhao, L., Ji, S., Long, T., Huang, Y., Ju, R., Tang, W., Tian, W., and Long, J. (2021). CircRNA-23525 regulates osteogenic

differentiation of adipose-derived mesenchymal stem cells via miR-30a-3p. Cell Tissue Res. 383, 795–807.

34. Zhao, X., Li, J., Zhao, S., Chen, L., Zhang, M., Ma, Y., and Yao, D. (2023). Regulation of bta-miRNA29d-3p on Lipid Accumulation via GPAM in Bovine Mammary Epithelial Cells. Mol. Biol. 13, 501–502.

35. King, O.D., Foulger, R.E., Dwight, S.S., White, J.V., and Roth, F.P. (2003). Predicting gene function from patterns of annotation. Genome Res. 13, 896–904.

36. Xu, X., Zhang, J., Tian, Y., Gao, Y., Dong, X., Chen, W., Yuan, X., Yin, W., Xu, J., Chen, K., et al. (2020). CircRNA inhibits DNA damage repair by interacting with host gene. Mol. Cancer 19, 128.

37. Li, X., Ao, J., and Wu, J. (2017). Systematic identification and comparison of expressed profiles of lncRNAs and circRNAs with associated co-expression and ceRNA networks in mouse germline stem cells. Oncotarget 8, 26573–26590.

38. Gu, X., Li, M., Jin, Y., Liu, D., and Wei, F. (2017). Identification and integrated analysis of differentially expressed lncRNAs and circRNAs reveal the potential ceRNA networks during PDLSC osteogenic differentiation. BMC Genet. 18, 100.

39. Wei, J., Li, M., Xue, C., Chen, S., Zheng, L., Deng, H., Tang, F., Li, G., Xiong, W., Zeng, Z., and Zhou, M. (2023). Understanding the roles and regulation patterns of circRNA on its host gene in tumorigenesis and tumor progression. J. Exp. Clin. Cancer Res. 42, 86.

40. Huang, C., Zhang, Y., Gong, Z., Sheng, X., Li, Z., Zhang, W., and Qin, Y. (2006). Berberine inhibits 3T3-L1 adipocyte differentiation through the PPARgamma pathway. Biochem. Biophys. Res. Commun. 348, 571–578.

41. Calejman, C.M., Doxsey, W.G., Fazakerley, D.J., and Guertin, D.A. (2022). Integrating adipocyte insulin signaling and metabolism in the multi-omics era. Trends Biochem. Sci. 47, 531–546.

42. Raza, S.H.A., Khan, R., Cheng, G., Long, F., Bing, S., Easa, A.A., Schreurs, N.M., Pant, S.D., Zhang, W., Li, A., and Zan, L. (2022). RNA-Seq reveals the potential molecular mechanisms of bovine KLF6 gene in the regulation of adipogenesis. Int. J. Biol. Macromol. 195, 198–206.

43. Lu, Q., Liu, T., Feng, H., Yang, R., Zhao, X., Chen, W., Jiang, B., Qin, H., Guo, X., Liu, M., et al. (2019). Circular RNA circSLC8A1 acts as a sponge of miR-130b/miR-494 in suppressing bladder cancer progression via regulating PTEN. Mol. Cancer 18, 111.

44. Friedrich, C.A. (2001). Genotype-phenotype correlation in von Hippel-Lindau syndrome. Hum. Mol. Genet. 10, 763–767.

45. Nadler, J.J., Zou, F., Huang, H., Moy, S.S., Lauder, J., Crawley, J.N., Threadgill, D.W., Wright, F.A., and Magnuson, T.R. (2006). Large-scale gene expression differences across brain regions and inbred strains correlate with a behavioral phenotype. Genetics 174, 1229–1236.

46. Wang, S., Yang, C., Pan, C., Feng, X., Lei, Z., Huang, J., Wei, X., and Ma, Y. (2022). Identification of key genes and functional enrichment pathways involved in fat deposition in Xinyang buffalo by WGCNA. Gene 818, 146225.

47. Hall, N.G., and Schönfeldt, H.C. (2013). Total nitrogen vs. amino-acid profile as indicator of protein content of beef. Food Chem. 140, 608–612.

48. Yuhong, G., Xue, F., Shuzhe, W., Hu, C., Li, F., Zhang, L., Yang, R., and Mayun. (2023). Function of circCAP2 in the Differentiation of Cattle (Bos taurus) Preadipocytes. J. Agricultural Biotechnol. *31*, 1441–1449.

49. Hu, C., Feng, X., Ma, Y., Wei, D., Zhang, L., Wang, S., and Ma, Y. (2023). CircADAMTS16 Inhibits Differentiation and Promotes Proliferation of Bovine Adipocytes by Targeting miR-10167-3p. Cells *12*, 1175.

50. Lv, S., Ma, M., Sun, Y., Wang, X., Qimuge, N., Qin, J., and Pang, W. (2017). MicroRNA-129-5p inhibits 3T3-L1 preadipocyte proliferation by targeting G3BP1. Anim. Cells Syst. *21*, 269–277.

51. Gentile, A.M., Lhamyani, S., Coín-Aragüez, L., Clemente-Postigo, M., Oliva Olivera, W., Romero-Zerbo, S.Y., García-Serrano, S., García-Escobar, E., Zayed, H., Doblado, E., et al. (2019). miR-20b, miR-296, and Let-7f Expression in Human Adipose Tissue is Related to Obesity and Type 2 Diabetes. Obesity *27*, 245–254.

52. Mærkedahl, R.B., Frøkiær, H., Lauritzen, L., and Metzdorff, S.B. (2015). Evaluation of a low-cost procedure for sampling, long-term storage, and extraction of RNA from blood for qPCR analyses. Clin. Chem. Lab. Med. *53*, 1181–1188.

53. You, X., and Conrad, T.O. (2016). Acfs: accurate circRNA identification and quantification from RNA-Seq data. Sci. Rep. *6*, 38820.

54. Giraldez, M.D., Spengler, R.M., Etheridge, A., Godoy, P.M., Barczak, A.J., Srinivasan, S., De Hoff, P.L., Tanriverdi, K., Courtright, A., Lu, S., et al. (2018). Comprehensive multi-center assessment of small RNA-seq methods for quantitative miRNA profiling. Nat. Biotechnol. *36*, 746–757.

55. Benesova, S., Kubista, M., and Valihrach, L. (2021). Small RNA-sequencing: approaches and considerations for miRNA analysis. Diagnostics *11*, 964.

56. Anders, S., and Huber, W. (2012). Differential Expression of RNA-Seq Data at the Gene Level–The DESeq Package, *10* (European Molecular Biology Laboratory (EMBL)), f1000research.

57. Conway, J.R., Lex, A., and Gehlenborg, N. (2017). UpSetR: an R package for the visualization of intersecting sets and their properties. Bioinformatics *33*, 2938–2940.

58. Conesa, A., Madrigal, P., Tarazona, S., Gomez-Cabrero, D., Cervera, A., McPherson, A., Szcześniak, M.W., Gaffney, D.J., Elo, L.L., Zhang, X., and Mortazavi, A. (2016). A survey of best practices for RNA-seq data analysis. Genome Biol. *17*, 13–19.

59. Iancu, O.D., Colville, A., Oberbeck, D., Darakjian, P., McWeeney, S.K., and Hitzemann, R. (2015). Cosplicing network analysis of mammalian brain RNA-Seq data utilizing WGCNA and Mantel correlations. Front. Genet. *6*, 174.

60. Hsu, S.-D., Chu, C.-H., Tsou, A.-P., Chen, S.-J., Chen, H.-C., Hsu, P.W.-C., Wong, Y.-H., Chen, Y.-H., Chen, G.-H., and Huang, H.-D. (2008). miRNAMap 2.0: genomic maps of microRNAs in metazoan genomes. Nucleic Acids Res. *36*, D165–D169.

61. Doncheva, N.T., Morris, J.H., Gorodkin, J., and Jensen, L.J. (2019). Cytoscape StringApp: network analysis and visualization of proteomics data. J. Proteome Res. *18*, 623–632.

62. Hulsegge, I., Kommadath, A., and Smits, M.A. (2009). Globaltest and GOEAST: Two Different Approaches for Gene Ontology Analysis (BioMed Central), pp. 1–5.

63. Flaherty, S.E., Grijalva, A., Xu, X., Ables, E., Nomani, A., and Ferrante, A.W. (2019). A lipase-independent pathway of lipid release and immune modulation by adipocytes. Science *363*, 989–993.

64. Kang, K., Peng, X., Luo, J., and Gou, D. (2012). Identification of circulating miRNA biomarkers based on global quantitative real-time PCR profiling. J. Anim. Sci. Biotechnol. *3*, 4–9.

65. Cohen, I., Huang, Y., Chen, J., Benesty, J., Benesty, J., Chen, J., Huang, Y., and Cohen, I. (2009). Pearson correlation coefficient. In Noise Reduction in Speech Processing, J. Benesty, ed. (Springer Science & Business Media), pp. 1–4.

66. Wang, G.H., Wang, S.H., Zhang, W.Z., Liang, C.C., Cheng, G., Wang, X.Y., Zhang, Y., and Zan, L.S. (2022). Analysis of stability of reference genes for qPCR in bovine preadipocytes during proliferation and differentiation *in vitro*. Gene *830*, 146502.

STAR★METHODS

KEY RESOURCES TABLE

REAGENT or RESOURCE	SOURCE	IDENTIFIER
Biological samples		
Three adult Jiaxian red cattle	Jiaxian Shanniu Breeding Limited Liability Company, Pingdingshan City, Henan Province, China	https://aiqicha.baidu.com/ company_basic_39302762533147
Critical commercial assays		
Illumina HiSeq 2500 sequencing	Shanghai Liebing Biomedical Technology CoChina,	https://www.novelbio.com
RNA Extraction Kit	Ambion,China	Cat#12183555CN
qRT-PCR kit	TaKaRa,China	Cat#RR047A
Deposited data		
Small RNA sequencing of seven different tissues (heart, liver, spleen, lung, kidney, muscle, and fat) of Jiaxian Red cattle	Sequence Read Archive	Database: PRJNA1000257
Complete Transcriptome sequencing of seven different tissues of Jiaxian Red Cattle (heart, liver, spleen, lung, kidney, muscle, fat)	Sequence Read Archive	Database: PRJNA1000105
Experimental models: Organisms/strains		
Bovine reference genome	Ensembl	Bos_taurus.ARS-UCD1.2.101.gtf
Software and algorithms		
miRNA identification(HISAT2)	{Giraldez, 2018 #83}{Benesova, 2021 #67}	http://daehwankimlab.github.io/ hisat2/download/
circRNA identification(HISAT2)	{You, 2016 #123}	http://daehwankimlab.github.io/ hisat2/download/
R 4.0.3	https://www.R-project.org/	N/A
Differential Expression Analysis(DESeq2)	{Anders, 2012 #135}	https://bioconductor.org/packages/release/ bioc/html/DESeq2.html
Differential gene upsets analysis(upsetR)	{Conway, 2017 #136}	https://github.com/hms-dbmi/UpSetR
Weighted Gene Co-Expression Network Analysis(WGCNA)	{Iancu, 2015 #95}	https://horvath.genetics.ucla.edu/html/ CoexpressionNetwork/Rpackages/WGCNA/ index.html
TargetScan	{Hsu, 2007 #89}	https://www.targetscan.org/ vert_72/docs/help.html
miRanda	operating environment:linux python=2.7.3	http://cbio.mskcc.org/microrna_data/ miRanda-aug2010.tar.gz
RNAhybird	operating environment:linux python=2.7.3	https://bibiserv.cebitec.uni
Cytoscape	{Doncheva, 2018 #76}	https://cytoscape.org/
GO/KEGG	{Hulsegge, 2009 #94}	https://david.ncifcrf.gov/
corrplotR	{Cohen, 2009 #72}	R package
GraphPad Prism	GraphPad Prism version 7	www.graphpad.com
Other		
Upstream and downstream analysis code related to RNAseq (personal blog)	github	https://wsz1207.github.io/

RESOURCE AVAILABILITY

Lead contact

Further information and requests for resources and reagents should be directed to and will be fulfilled by the Lead Contact, Dr. Yun Ma. (mayun_666@126.com).

Materials availability

No new unique reagents were generated.

Data and code availability

The original sequencing file has been uploaded to the SRA server of NCBI. Jiaxian red cattle Full Transcriptome Database: PRJNA1000105; Jiaxian red cattle Small RNA Database: PRJNA1000257.

   This paper does not report original code.

   Any additional information required to reanalyze the data reported in this paper is available from the lead contact upon request.

EXPERIMENTAL MODEL AND STUDY PARTICIPANT DETAILS

Animals

Three adult male Jiaxian red cattle, aged 36 months, belonging to the Bos taurus (ID: 9913) species. Additionally, in beef quality research, the utilization of bulls (male) is more common than that of cows (female). This is because, apart from specific breeding bulls, cows are also engaged in calving, making them less common for fattening and slaughter purposes.

Ethics statement

Animal experiments were conducted following the Regulations for the Administration of Affairs Concerning Experimental Animals. The Animal Ethics Committee approved them of Ningxia University (NXU20180607) (Figure S5).

METHOD DETAILS

Sample acquisition and total RNA extraction

Heart, spleen, lung, liver, brain, kidney, longest dorsal muscle and dorsal subcutaneous adipose tissue were collected from three adult Jiaxian red bulls. Tissue samples were lysed using TRIzol reagent (Ambion, Life Technologies, NY), and then total RNA was extracted according to the manufacturer's protocol (Invitrogen, Carlsbad, CA). Enzyme marker (synergy|LX, BioTek) was used to determine the concentration and integrity of RNA.[52] Total RNA was stored at -80°C for subsequent experiments.

QUANTIFICATION AND STATISTICAL ANALYSIS

Identification and differential expression analysis of non-coding RNAs in Jiaxian red cattle

The experiment employed the Illumina HiSeq sequencing platform in paired-end mode for high-throughput sequencing of the samples. To identify circRNAs, specific criteria were adopted based on known circRNA structural and splicing sequence features. These criteria included GU/AG splice sites at the junction, allowing a maximum of 2 mismatches, and requiring a minimum of 2 reads at the junction within a total size of 100 kb.[53] Polished version: miRNA sequencing was performed using the Illumina HiSeq platform in single-end mode for high-throughput sequencing. To ensure data quality and accuracy, several filtering criteria were applied, including the removal of reads containing 3′ adapter sequences, reads with 'N' bases, and reads with low-quality base scores below specific thresholds. Additionally, reads with polyA/T sequences and reads with lengths outside the range of 15 to 40 bp were filtered out.[54,55]

   The differential analysis of circRNA expression was conducted using the DESeq package (Version 1.40.1) in R software (Version 4.05), considering the sample grouping and circRNA-miRNA expression TPM values.[56] For the selection of differentially expressed genes, the UpSetR software (Version 1.4.0) was utilized.[57] The differentially expressed non-coding RNAs were identified based on a rigorous filtering criterion of Log2foldchange $\geq$ 1.7 and a P-value threshold of < 0.05, considering biological replicate samples.[58]

Weighted gene co-expression network analysis (WGCNA)

In this study, the R package WGCNA (Version 1.69) was utilized for constructing co-expression networks. Absolute median difference expression and genes with TPM values greater than 1 were employed for co-expression network analysis. The blockwiseModules function from the WGCNA package was used for the one-step construction of the co-expression network. Subsequently, the labeled Heatmap function was employed to perform correlation analysis between phenotype and gene expression data, aiming to identify significantly correlated co-expression modules. The filtering criteria for module selection were set as r $\geq$ 0.8 and p < 0.01. After selecting key modules, genes with significant gene significance (|GS| $\geq$ 0.4) and module membership (|MM| $\geq$ 0.4) were chosen as key genes for further analysis.[59]

Non-coding RNA mechanism prediction and functional enrichment analysis

The analysis of circRNA-miRNA interactions involved the use of RNAHybrid (Version 2.1.2) and miRanda (Version 2.042) tools in the Linux system. The prediction of miRNA-targeted mRNAs was carried out utilizing RNAHybrid (Version 2.1.2), miRanda (Version 2.042), and the web-based version of TargetScan (https://www.targetscan.org/vert_72/docs/help.html).[60] The construction of an interaction network between non-coding RNAs and mRNAs was accomplished using Cytoscape software (Version 9.2).[61] Furthermore, the predicted mRNAs underwent Gene Ontology (GO) and Kyoto Encyclopedia of Genes and Genomes (KEGG) pathway analysis and visualization using the clusterProfiler package in R software (Version 4.0.5).[62,63]

Identification of non-coding RNA by qRT PCR and association analysis with amino acids

Specific primers were designed to identify the junction sequences of circRNA by targeting the ends of the adapter sites. Primer pairs were constructed at the ends of circRNA adapter sites for circRNA identification using real-time quantitative PCR (qRT-PCR). Universal loop primers and quantitative primers were designed for miRNA reverse transcription and quantification. The PrimeScript™ RT reagent Kit miRNA (TaKaRa) (RR047A) was used for circRNA and miRNA reverse transcription.[64] Real-time quantitative PCR (qRT-PCR) was performed using the TaKaRa quantitative kit on a LightCycler® 96 instrument (Roche, Germany) to measure the expression levels of non-coding RNAs. All primers used are listed in Table S1.

Pearson correlation analysis was used to study the relationship between key genes and amino acid content in the muscles of Jiaxian red cattle. The results obtained were visualized using the R package corrplot (version = 0.90) in the R package. where $|r| \in (0, 0.33)$ is a weak correlation, $|r| \in [0, 0.66)$ is a moderate correlation, $|r| \in [0.66, 1]$ is a strong correlation, "*" stands for $p < 0.05$, "**" stands for $p < 0.01$, and "***" stands for $p < 0.001$.[65]

Statistical tests

Statistical significance of non-coding RNA expression across seven tissues was analyzed using non-parametric tests or t-tests based on the distribution characteristics of the data. GAPDH expression level was used as the reference for circRNA detection, while U6 expression level served as the reference for miRNA examination.[66] The relative expression levels of genes were calculated using the $2^{-\Delta\Delta Ct}$ method, and a P-value < 0.05 was considered statistically significant. The letter 'n' signifies the quantity of animals, while 'SD' represents the mean value.